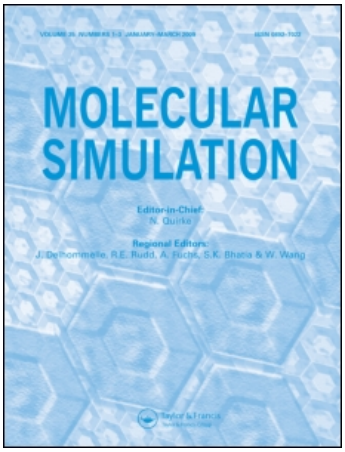

Molecular Simulation
Publication details, including instructions for authors and subscription information:
http://www.informaworld.com/smpp/title~content=t713644482

Monte Carlo Simulation of Fluids in Curved Three-dimensional Space

Lisa A. Fanti[a]; Eduardo D. Glandt[a]
[a] Department of Chemical Engineering, University of Pennsylvania, Philadelphia, PA, USA

To cite this Article Fanti, Lisa A. and Glandt, Eduardo D.(1989) 'Monte Carlo Simulation of Fluids in Curved Three-dimensional Space', Molecular Simulation, 2: 3, 163 — 176
To link to this Article: DOI: 10.1080/08927028908031365
URL: http://dx.doi.org/10.1080/08927028908031365

Molecular Simulation, 1989, Vol. 2, pp. 163–176
Reprints available directly from the publisher
Photocopying permitted by license only

MONTE CARLO SIMULATION OF FLUIDS IN CURVED THREE-DIMENSIONAL SPACE

LISA A. FANTI and EDUARDO D. GLANDT

Department of Chemical Engineering, University of Pennsylvania, Philadelphia, PA 19104, USA

(*Received April 1988; in final form July 1988*)

This work describes the methods required to perform computer simulations of three-dimensional fluids confined to the surface of a four-dimensional hypersphere. The use of such non-Euclidian spaces, or spherical boundary conditions, is convenient in cases where spatial inhomogeneities occur over length-scales comparable to that of the entire system. The form of the pressure equation in curved space is discussed, and the results of Monte Carlo simulations of hard spheres confined to the surface of a hypersphere are presented. Comparison of the simulation results to the Carnahan-Starling equation of state in flat space provides a basis for determining when curvature effects can be neglected.

KEY WORDS: Curved space, equation of state, hard spheres, Monte Carlo, non-Euclidian space.

1 INTRODUCTION

Model classical fluids embedded in curved spaces have been proposed in recent years to exploit some of the advantages of non-Euclidian geometry. Kratky [1] suggested the use of curved spaces to implement "spherical" boundary conditions in the computer simulation of dense fluids. These conditions offer an alternative to the traditional, almost exclusive use of toroidal boundary conditions, in which a finite Euclidian system is surrounded by replicas of itself to create a pseudo-infinite arrangement. The main purpose of both of these periodic-type boundary conditions is to eliminate edge effects. In either case, some long-ranged correlations are introduced into the statistics gathered during a simulation.

There exist situations in which toroidal boundary conditions are not the most convenient. Prominent among such cases are simulations involving very large spatial inhomogeneities in an applied field, or very large particles, comparable to the size of the system being simulated. The simulation of high polymers, or of fluids embedded in a matrix of fibers [2] that must necessarily span the system, are two examples. In these cases, toroidal boundary conditions impose too restrictive a constraint on the allowable configurations, and might be altogether impossible to implement. Spherical boundary conditions, based on "wrapping" a D-dimensional system over the surface of a $D + 1$ dimensional sphere, are an appropriate alternative. Although they introduce curvature into the system, they permit the easy construction of configurations free from edges and other discontinuities. Figure 1 illustrates the advantages of spherical boundary conditions for a two-dimensional fibrous structure. In addition, curved space may be used in simulations in order to inhibit crystallization [3]. This facilitates the study of phase transitions from a metastable liquid, such as the formation of glasses, which might otherwise be difficult to observe.

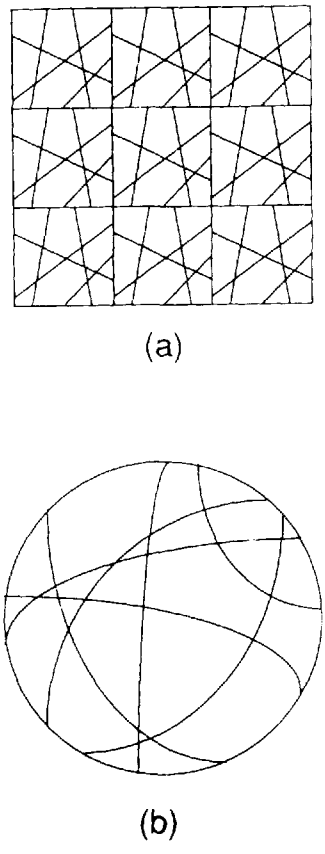

Figure 1 (a) Toroidal boundary conditions do not eliminate edge effects for a two-dimensional fibrous network. (b) Wrapping this system around a three dimensional sphere eliminates edge effects.

In some applications, the results of studies in curved spaces have been extrapolated to zero curvature to yield the corresponding properties in flat, Euclidian space. Other work has focused on systems of large curvature. Kratky and co-workers [1, 4] have presented some general results for systems of D-dimensional particles confined to the surface of a $D + 1$ dimensional sphere, and performed Monte Carlo simulations for the 12-6 Lennard-Jones model in three dimensions. These were used to extract the leading corrections in an expansion of the thermodynamic properties of the fluid in powers of the curvature. Other than in this work, the use of spherical boundary conditions has largely been restricted to two-dimensional curved space. Kratky [1] and Post and Glandt [5] have used a virial expansion to study the properties of hard spheres (hard caps) adsorbed onto the surface of a three-dimensional sphere. This model has applications to several physical systems, including the adsorption of gases in molecular-sieve cavities and of biological molecules onto spherical substrates. Post and Glandt [5] have also discussed the alternative forms of the pressure equation for

such systems, and performed Monte Carlo simulations to obtain the pressure and activity coefficient for a hard-cap fluid.

The present work is concerned with the simulation techniques needed to study systems embedded in a three-dimensional space of large positive curvature, i.e. confined to the surface of a four-dimensional hypersphere. An obvious complication when working in curved space of three dimensions is the non-intuitive nature of the geometry, and the impossibility of visualizing the configurations of the particles. Here, the coordinate systems and other appropriate methods to facilitate such simulations are discussed. The calculation of thermodynamic properties, in particular the form of the pressure equation and the virial coefficients, is also considered.

An additional objective of this work is to obtain an indication of the size of the system for which curvature effects on the thermodynamic properties become negligible. To this end, Monte Carlo simulations are used to calculate the pressure and the chemical potential of a hard-sphere fluid in curved space. These results are compared to the predictions of the Carnahan-Starling equation of state for Euclidian hard spheres to help quantify curvature effects.

The following section introduces the geometry necessary to describe a system of spherical particles in curved space. Section 3 contains the forms of the pressure equation for particles interacting through both a curved line of force and a Euclidian line of force. In Section 4, the second and third virial coefficients for hard spheres confined to a hypersphere are calculated. The Monte Carlo simulation methods are presented in Section 5, and discussed in Section 6.

2 GEOMETRY ON A FOUR-DIMENSIONAL HYPERSPHERE

The equation for a hypersphere of radius R in Cartesian coordiantes is

$$x^2 + y^2 + z^2 + t^2 = R^2 \tag{1}$$

It is instructive to introduce several coordinate systems, which will be used in the derivations that follow. The transformation to hyperspherical coordinates (R, p, q, r) is given by [6]

$$\begin{aligned} x &= R \sin p \sin q \\ y &= R \sin p \cos q \\ z &= R \cos p \cos r \\ t &= R \cos p \sin r \end{aligned} \tag{2}$$

where $0 < p < \pi/2$, $0 < q < 2\pi$, and $0 < r < 2\pi$. The differential element of (three-dimensional) volume on the hypersurface is

$$dV = \frac{R^3}{2} d(\sin^2 p)\, dq\, dr \tag{3}$$

so that the total volume of the system is $2\pi^2 R^3$. On a hypersphere of unit radius, the Cartesian coordiantes are the direction cosines. The angular separation between two points, which must be computed frequently during a simulation, is obtained from the inner product of their direction vectors

$$\cos \xi = \sin p_1 \sin p_2 [\cos (q_2 - q_1)] + \cos p_1 \cos p_2 [\cos (r_2 - r_1)] \quad (4)$$

Although this coordinate system is the only one required during the course of a simulation, it is not spherically symmetric, i.e. none of its coordinate surfaces is a locus of points equidistant from another point. A symmetric system is used in the normalization of the particle-particle distances to compute the pair correlation function, for example. For such purposes, two additional coordinate transformations will be introduced. First, all points on the curved three-dimensional surface of the hypersphere may be mapped onto a three-dimensional Euclidian space (u, v, w) by

$$\begin{aligned} x &= \frac{2R^2 u}{R^2 + u^2 + v^2 + w^2} \\ y &= \frac{2R^2 v}{R^2 + u^2 + v^2 + w^2} \\ z &= \frac{2R^2 w}{R^2 + u^2 + v^2 + w^2} \\ t &= \frac{R(R^2 - u^2 - v^2 - w^2)}{R^2 + u^2 + v^2 + w^2} \end{aligned} \quad (5)$$

This transformation is better understood by considering its three-dimensional analog: the mapping of all points on the surface of a sphere onto the equatorial plane (i.e. two-dimensional Euclidian space) by projection through the south pole. The first transformation is followed by a conversion to spherical coordinates (ϱ, θ, ϕ) in Euclidian space

$$\begin{aligned} \frac{u}{R} &= \varrho \sin\theta \cos\phi \qquad \text{where} \qquad 0 < \varrho < \infty \\ \frac{v}{R} &= \varrho \sin\theta \sin\phi \qquad\qquad 0 < \theta < \pi \\ \frac{w}{R} &= \varrho \cos\theta \qquad\qquad 0 < \phi < 2\pi \end{aligned} \quad (6)$$

Let ξ designate the angular distance of a point on the surface of the hypersphere to the angular origin (the "north pole"). This hyper-longitude is given by $\sin \xi = 2\varrho/(1 + \varrho^2)$. The volume of a differential element on the surface of the hypersphere is

$$dV = R^3 \sin\theta \, d\theta \, d\phi \, \sin^2\xi \, d\xi \quad (7)$$

The volume of a sphere of angular diameter α embedded in three-dimensional curved space is obtained by integration over the angles θ and ϕ, and over ξ from 0 to the particle angular radius $\alpha/2$. The packing fraction η is therefore given by

$$\eta = \frac{N}{2\pi} [\alpha - \sin\alpha] \quad (8)$$

This can be compared to its limit as α $(= a/R) \to 0$, i.e. to $\eta = \pi(N/V)a^3/6$ in Euclidian space.

3 EQUATION OF STATE

An intrinsic characteristic of systems confined to spaces of positive curvature is their finite size. Earlier work [7, 8] has addressed the effects of finite system size on the statistical mechanics of fluids. Usually, the thermodynamic limit refers to a hypothetical system with an infinite volume and an inifinite number of particles. Hill [9] showed that the thermodynamics of small systems are also well defined by considering a special ensemble of replicas of a canonical system. He showed that in such cases the intensive properties remain dependent upon both the number of particles N, and the size and shape of the volume V individually, and not just on their ratio, the number density of particles. Also, the fact that the number of particles can only change by a discrete amount becomes significant for a small system. The fundamental differential relation for the Helmholtz free energy of a pure substance must be written as

$$\delta F = -S\,dT - p\,dV + \mu\,\Delta N \tag{9}$$

where the pressure is simply

$$p_N = \left[\frac{\partial F}{\partial V}\right]_{T,N} \tag{10}$$

In the present case, this corresponds to an isotropic expansion of the hypersphere. The chemical potential is defined as

$$\mu_N = \left[\frac{\delta F}{\Delta N}\right]_{T,V} = F_N - F_{N-1} \tag{11}$$

The configurational integral for N spherical particles adsorbed onto the surface of a hypersphere is given by

$$Z_N = \left(\frac{V}{2\pi^2}\right)^N \int e^{-u/kt} \sin\theta_1\,d\phi_1 \sin^2\xi_1\,d\xi_1 \ldots \sin\theta_N\,d\theta_N\,d\phi_N \sin^2\xi_N\,d\xi_N \tag{12}$$

Equations (10) and (12) yield

$$\frac{p_N}{kT} = \left(\frac{N}{V}\right) - \frac{1}{kT}\left(\frac{N}{V}\right)^2 \frac{V}{3\pi} \int_0^\pi R\left[\frac{\partial u}{\partial R}\right]_\xi g(\xi) \sin^2\xi\,d\xi \tag{13}$$

where ξ is the angular interparticle separation, u is the pair-wise interaction potential and $g(\xi)$ is the pair correlation function

$$g(\xi) = \frac{V^2 R^{3N-6}}{Z_N}\left[1 - \frac{1}{N}\right] \int e^{-U/kT} \sin\theta_3\,d\theta_3\,d\phi_3 \sin^2\xi_3\,d\xi_3 \ldots \times$$
$$\sin\theta_N\,d\theta_N\,d\phi_N \sin^2\xi_N\,d\xi_N \tag{14}$$

As discussed by Post and Glandt [5], the factor $\partial u/\partial R$ depends upon the nature of the energetic interactions between particles. Two possibilities arise, depending on whether these interactions occur within the curved space of D dimensions or within a flat space of $D + 1$ dimensions. In the first of these, termed the "curved line of force" case, the natural metric for interparticle distances is the arc length separating two particles, $l = R\xi$. In the second case, that of the "Euclidian line of force," attractions or repulsions occur along the straight line in $D + 1$ dimensional space between two particles, the chord of length $z = 2R \sin(\xi/2)$. This circumstance corresponds to

particles interacting *through* the inside of the hypersphere, and has no obvious physical significance here, unlike the adsorption applications of the development of Post and Glandt. For the curved line of force assumption

$$\left[\frac{\partial u}{\partial R}\right]_l = 0 \tag{15}$$

so that the isotropic expansion of the hypersphere obeys

$$\left[\frac{\partial u}{\partial R}\right]_\xi = \xi\left[\frac{\partial u}{\partial l}\right]_R \tag{16}$$

In this instance the pressure is given by

$$\frac{p_N^e}{kT} = \left(\frac{N}{V}\right) - \frac{2\pi R^3}{3}\frac{1}{kT}\left(\frac{N}{V}\right)^2 \int_0^\pi \left[\frac{\partial u}{\partial \xi}\right]_R g(\xi)\,\xi\,\sin^2\xi\,d\xi \tag{17}$$

For hard particles, the pressure equation becomes

$$\frac{p_N^e V}{NkT} = 1 + \frac{2\pi R^3}{3}\left(\frac{N}{V}\right) g(\alpha)\,\alpha\,\sin^2\alpha \tag{18}$$

This result was reported by Kratky [1]. For the sake of completeness, we also consider the Euclidian line-of-force assumption, in which the straight linear diameter of the particles and not their angular diameter remains constant upon an isotropic expansion of the hypersphere. Thus

$$\left[\frac{\partial u}{\partial R}\right]_z = 0 \tag{19}$$

so that

$$\left[\frac{\partial u}{\partial R}\right]_\xi = 2\sin(\xi/2)\left[\frac{\partial u}{\partial z}\right]_R \tag{20}$$

and the pressure equation is given by

$$\frac{p_N^e}{kT} = \left(\frac{N}{V}\right) - \frac{8\pi R^3}{3}\frac{1}{kT}\left(\frac{N}{V}\right)^2 \int_0^\pi \left[\frac{\partial u}{\partial \xi}\right]_R g(\xi)\,\sin^2(\xi/2)\,\sin\xi\,d\xi \tag{21}$$

For hard spheres, Equation (21) becomes

$$\frac{p_N^e V}{NkT} = 1 + \frac{8\pi R^3}{3}\left(\frac{N}{V}\right) g(\alpha)\,\sin^2(\alpha/2)\,\sin\alpha \tag{22}$$

Pressures can be computed with either Equation (18) or (22) after obtaining the pair correlation function from Monte Carlo simulation. However, only the curved line-of-force approach, Equation (18), will be used in what follows.

4 VIRIAL EXPANSION

The coordinate systems presented in Section 2 are also appropriate for the calculation of the virial coefficients. The compressibility factor may be expanded as

$$\frac{pV}{NkT} = 1 + \sum_{n=2}^{\infty} B_n \left(\frac{N}{V}\right)^{n-1} \tag{23}$$

Unlike in the case of an infinite system, the virial coefficients for a finite system remain explicitly dependent on the number of particles and on the size and shape of the volume. The complete dependence was presented by Kratky [1]. The second and third virial coefficients are

$$B_2(N, V) = \left(1 - \frac{1}{N}\right) B_2(V) \tag{24}$$

and

$$B_3(N, V) = \left(1 - \frac{1}{N}\right)\left(1 - \frac{2}{N}\right) B_3(V) + \frac{2}{N}\left(1 - \frac{1}{N}\right) B_2^+(V)\, B_2(V) \tag{25}$$

For a three-dimensional hard sphere fluid in curved space, the volume-dependent parts are

$$B_2(V) = B_2\left[\frac{\sin\alpha}{\alpha}\right]^2 \tag{26}$$

$$B_3(V) = R^3\, y_1(\alpha, \alpha)\, B_2(V) \tag{27}$$

$$B_2^+(V) = \frac{3\, B_2}{\alpha}\left[\frac{2\alpha - \sin 2\alpha}{(2\alpha)^2}\right] \tag{28}$$

where $B_2 = 2\pi(\alpha R)^3/3$. The factor $R^3 y_1(\xi, \alpha)$ appearing in the expression for $B_3(V)$ is the intersection volume of two spheres of angular *radius* α at a center-to-center angular separation ξ. The determination of $y_1(\alpha, \alpha)$ entails an integration over the domain common to both spheres. It is convenient to consider two hard spheres situated at

$$\{p_1, q_1, r_1\} = \left\{0, 0, \frac{\pi}{2} - \frac{\alpha}{2}\right\}$$

and (29)

$$\{p_2, q_2, r_2\} = \left\{0, 0, \frac{\pi}{2} + \frac{\alpha}{2}\right\}$$

Each sphere is defined by the locus of points which are α-equidistant from the above coordinates. Equation (4) shows the two representative equations to be

$$\cos\alpha = \cos p \sin r \cos\frac{\alpha}{2} + \cos p \cos r \sin\frac{\alpha}{2}$$

and

$$\cos\alpha = \cos p \sin r \cos\frac{\alpha}{2} - \cos p \cos r \sin\frac{\alpha}{2} \tag{30}$$

The choice of coordinates in Equation (29) is not arbitrary. Imposing the coordinate transformations given in Equations (5) and (6) serves to map the two curved spheres in non-Euclidian space onto two equisized spheres in the Euclidian (u, v, w) space, symmetric about the origin

$$u^2 + v^2 + (w-w_o)^2 = R_o^2 R^2$$

and

$$u^2 + v^2 + (w+w_o)^2 = R_o^2 R^2 \tag{31}$$

where

$$w_o = \frac{\sin\frac{\alpha}{2}}{\cos\frac{\alpha}{2} + \cos\alpha} R \tag{32}$$

and

$$R_o = \left[\frac{\cos\frac{\alpha}{2} - \cos\alpha}{\cos\frac{\alpha}{2} + \cos\alpha} + \frac{\sin^2\frac{\alpha}{2}}{\left(\cos\frac{\alpha}{2} + \cos\alpha\right)^2}\right]^{1/2} \tag{33}$$

Invoking the transformation to spherical coordinates as in Equation (6), the differential volume element

$$dV = \frac{8R^3\varrho^2}{(1+\varrho^2)^3} d\varrho \sin\theta \, d\theta \, d\phi \tag{34}$$

can be integrated over one octant of the domain common to both spheres; i.e. over

$$0 < \phi < \frac{\pi}{2} \tag{35}$$

$$0 < \varrho(\theta) < -\frac{w_o}{R}\cos\theta + \left[R_o^2 - \sin^2\theta\left(\frac{w_o}{R}\right)^2\right]^{1/2}$$

$$0 < \theta < \frac{\pi}{2}$$

Table I shows $y_1(\alpha, \alpha)$, as determined by numerical integration of Equation (34). These results can be used to compute the third virial coefficient for any number of particles and system size.

5 MONTE CARLO SIMULATION METHODS

Monte Carlo computer simulations were carried out for three-dimensional hard spheres confined to the surface of a hypersphere. However, the same approach is also applicable to systems with any interparticle interaction. The conventional Metropolis canonical algorithm was used [10, 11], so that only those details specific to simulations in curved space are discussed here. As in all simulations, care was taken to move the particles in an unbiased fashion. In spherical geometries, moves must not favor either the poles or the equator, so that the fluid remains homogeneous. Equation (30) shows

Table 1 Intersection volume of two spheres of angular radius α and angular separation α in three-dimensional curved space.

α	y_i
0.0	0.0000 E + 00
0.1	1.3087 E − 03
0.2	1.0464 E − 02
0.3	3.5280 E − 02
0.4	8.3514 E − 02
0.5	1.6284 E − 01
0.6	2.8082 E − 01
0.7	4.4492 E − 01
0.8	6.6248 E − 01
0.9	9.4077 E − 01
1.0	1.2870 E + 00
1.1	1.7084 E + 00
1.2	2.2123 E + 00
1.3	2.8064 E + 00
1.4	3.4987 E + 00
1.5	4.2983 E + 00

that the following coordinates are uniformly distributed over the surface of the hypersphere

$$\begin{aligned} 0 &< \sin^2 p < 1 \\ 0 &< q < 2\pi \\ 0 &< r < 2\pi \end{aligned} \tag{36}$$

and were used in the displacement of the particles. The steps in the q and r directions were uniformly distributed in $[-\Delta, \Delta]$, where Δ is the maximum displacement, together with periodic boundary conditions. Movement along the $\sin^2 p$ direction used a different maximum displacement and involved reflective boundary conditions at $\sin^2 p = 0$ and 1. This procedure can be easily shown to obey detailed balance. Kratky and Schreiner [4a] have used an alternative approach based on an isotropic displacement of the particles.

To calculate the equation of state, given by Equation (18), the pair correlation function at contact is required. To obtain it, a histogram of interparticle separations was kept throughout the simulations. The coordinate system of Equation (2) was utilized to specify particle positions to facilitate the calculation of these separations. Intervals of equal volume were used in the preparation of the histogram, so that the same number of pairs would be encountered for all intervals in the case of noninteracting particles. Equation (7) indicates that the sectors must be divided as

$$\Delta V = \Delta\left[\xi - \frac{1}{2}\sin(2\xi)\right] \tag{37}$$

The chemical potential μ_N was evaluated using Widom's particle insertion technique [12]. The chemical potential can be expressed as

$$\mu_N = \mu_0 + kT \ln\left(V \frac{Z_{N-1}}{Z_N}\right) \tag{38}$$

The quantity in braces approaches unity in the low density limit and defines μ_o as the chemical potential of the particles in the ideal gas state at the same density. The appropriate definition for the fugacity or activity coefficient ϕ is therefore

$$\phi = V\left(\frac{Z_{N-1}}{Z_N}\right) \tag{39}$$

Widom [12] has shown that

$$\phi = \langle e^{-W/kT}\rangle^{-1} \tag{40}$$

where the quantity in brackets denotes an ensemble average of the Boltzmann factor for the interactions of the N-th particle with the other N-1. In the case of hard particles, this average becomes the fraction of times that the N-th particle can be successfully inserted into a typical configuration of N-1 particles.

6 RESULTS AND DISCUSSION

Simulations were performed for systems of 10, 20, 30, 40 and 50 particles at varying packing fractions. Such small system sizes were required to reveal curvature effects. The minimum number of moves per particle for all runs was 30,000. The number of attempted particle insertions per configuration necessary to obtain adequate statistics for the activity coefficients varied from 1 for 20% to 500 for 40% packing. The accuracy of the pressures and activity coefficients calculated by the simulations was estimated by the method of Kolafa [13]. The values of the pressure at three different packing fractions are shown in Table 2, as calculated from Equation (18). The number of decimal places reported is an indication of the estimated error. Pressures for systems of 10 and 50 particles are compared in Figure 2.

The solid lines in Figure 2 are the predictions for systems of 10 and 50 particles obtained from the virial expansion, using virial coefficients only through B_3. How-

Table 2 Compressibility factors calculated by Monte Carlo simulation. N is the number of particles, η is the packing fraction and α is the angular diameter subtended by a particle. The estimated error corresponds to the last decimal place reported.

N	η	α	pV/NkT
10	0.2	0.9232	2.164 ± 1
10	0.3	1.0618	3.29 ± 2
10	0.4	1.1734	5.41 ± 5
20	0.2	0.7288	2.250 ± 1
20	0.3	0.8366	3.47 ± 2
20	0.4	0.9232	5.77 ± 4
30	0.2	0.6354	2.274 ± 9
30	0.3	0.7288	3.51 ± 1
30	0.4	0.8038	5.85 ± 5
40	0.2	0.5766	2.301 ± 1
40	0.3	0.6612	3.53 ± 2
40	0.4	0.7288	5.79 ± 4
50	0.2	0.5348	2.294 ± 9
50	0.3	0.6132	3.58 ± 2
50	0.4	0.6758	5.87 ± 4

ever, the effects of higher-order terms were estimated using a two-point Padé-like approximant. This rational function

$$\frac{pV}{NkT} = 1 + \frac{B_2(N, V)\left(\frac{N}{V}\right) + \left[B_3(N, V) - \frac{V B_2(N, V)}{N_{max}}\right]\left(\frac{N}{V}\right)^2}{1 - (N/N_{max})} \tag{41}$$

yields the exact virial coefficients B_2 and B_3, and also reproduces the divergence in the pressure at the random close packing limit N_{max}. The required value of the close-packed density N_{max}/V in the curved space was obtained using the Euclidian packing fraction value of 0.64. Wille [14] has recently investigated the maximum packing fractions on the surface of a hypersphere using computer simulations, and has shown

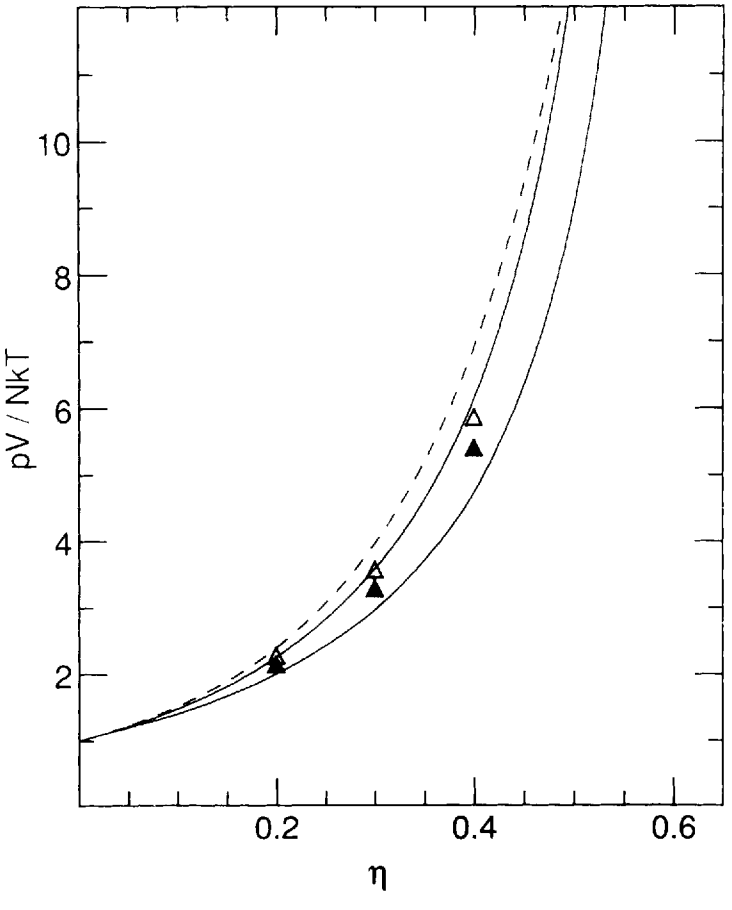

Figure 2 Compressibility factors as a function of the packing fraction, η. The filled and open triangles are Monte Carlo results for 10 and 50 particles, respectively. The solid lines are the corresponding rational approximants, Eq. (41). The dashed line is the Carnahan-Starling equation of state.

that it deviates very little from the Euclidian value for all but some special values of the curvature. The approximant does very well at lower packing fractions, and is reasonable over the range of densities considered here. Also shown in Figure 2 is the Carnahan-Starling equation of state [15] for hard spheres in Euclidian space

$$\frac{pV}{NkT} = \frac{1 + \eta + \eta^2 - \eta^3}{(1 - \eta)^3} \tag{42}$$

Deviation from this curve is the result of two effects: the curvature of the space and the finite size of the system. For a constant number of particles, Equation (8) shows how the angular diameter of the particles decreases with the packing fraction. This explains the better agreement with the Euclidian result at lower packing fractions. For a given packing density, the augular diameter decreases with an increase in the number of particles. As a result, the pressures for 50-particle systems deviate less than those for 10 particles at all densities. Figure 3 shows an interpolated diagram of the differences between the simulation pressures and the Carnahan-Starling values for the same packing fraction. This plot gives an indication of the order of magnitude of the curvature effects in the application of spherical boundary conditions.

The activity coefficients determined by the particle-insertion method for several particle numbers and coverages are shown in Table 3. These results show high uncertainties at high densities, even for an insertion rate of 500 per configuration. In Figure 4, the activity coefficients for 10 and 50 particles are compared to the flat-space result corresponding to the Carnahan-Starling equation

$$\ln \phi = \frac{8\eta - 9\eta^2 + 3\eta^3}{(1 - \eta)^3} \tag{43}$$

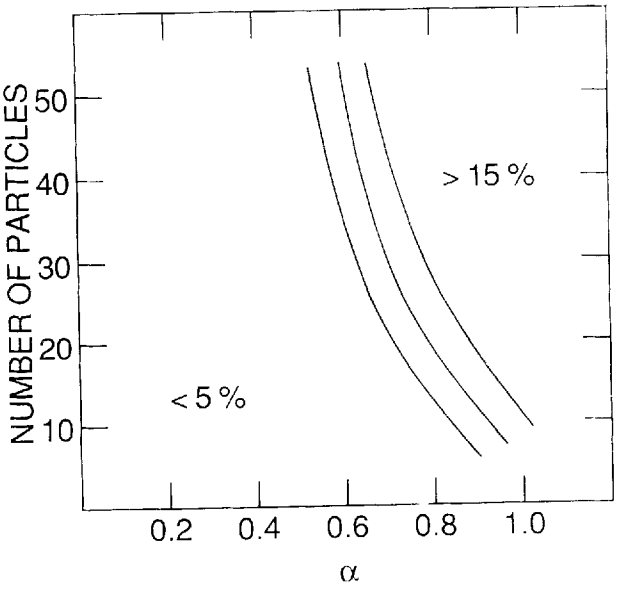

Figure 3 Interpolated diagram of the differences between the simulation pressures and the Carnahan-Starling value for the same packing fraction. The lines correspond to 5, 10, and 15% differences.

Table 3 Activity coefficients calculated by Monte Carlo simulation. The estimated error corresponds to the last decimal place reported.

N	η	α	$ln\ \phi$
10	0.2200	0.9232	2.242 ± 6
10	0.3300	1.0618	4.39 ± 1
10	0.4400	1.1734	8.31 ± 9
20	0.2100	0.7288	2.299 ± 6
20	0.3150	0.8366	4.54 ± 2
20	0.4200	0.9232	8.47 ± 8
30	0.2067	0.6354	2.328 ± 7
30	0.3100	0.7288	4.63 ± 2
30	0.4135	0.8038	8.76 ± 9
40	0.2050	0.5766	2.337 ± 8
40	0.3075	0.6612	4.69 ± 3
40	0.4100	0.7288	8.82 ± 9
50	0.2040	0.5348	2.352 ± 9
50	0.3060	0.6132	4.69 ± 2
50	0.4080	0.6758	8.57 ± 9

As expected, the largest system size and the lowest packing fractions are once again closest to the Euclidian result.

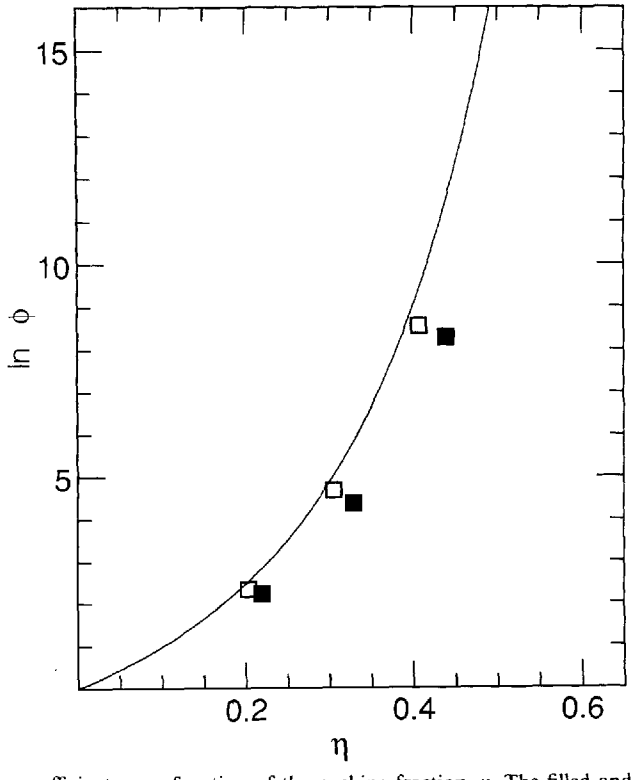

Figure 4 Activity coefficients as a function of the packing fraction, η. The filled and open squares are Monte Carlo results for 10 and 50 particles, respectively. The dashed line is the activity coefficient corresponding to the Carnahan-Starling equation of state.

Acknowledgments

Support from the Laboratory for Research on the Structure of Matter at the University of Pennsylvania is acknowledged. The authors are also grateful to the John von Neumann Center for the allocation of supercomputer time required for the performance of these simulations.

References

[1] K.W. Kratky, "New boundary conditions for computer experiments of thermodynamic systems," *J. Comput. Phys.*, **37**, 205 (1980).
[2] L.A. Fanti and E.D. Glandt, to be submitted (1988).
[3] D.R. Nelson, "Liquids and glasses in spaces of incommensurate curvature," *Phys. Rev. Lett.*, **50**, 982 (1983).
[4] K.W. Kratky and W. Schreiner, "Computational techniques for spherical boundary conditions," *J. Comput. Phys.*, **47**, 313 (1982); W. Schreiner and K.W. Kratky, "Finiteness effects in computer simulation of fluids with spherical boundary conditions," *Mol. Phys.*, **50**, 435 (1983).
[5] A.J. Post and E.D. Glandt, "Statistical thermodynamics of particles adsorbed onto a spherical surface," *J. Chem. Phys.*, **85**, 7349 (1986).
[6] A.R. Forsyth, *Geometry of Four Dimensions* (The University Press, Cambridge, 1930), Vols. 1 and 2.
[7] J.L. Lebowitz and J.K. Percus, "Thermodynamic properties of small systems," *Phys. Rev.*, **124**, 1673 (1961).
[8] J. Hubbard, "On the equation of state of small systems," *J. Chem. Phys.*, **55**, 1382 (1971).
[9] T.L. Hill, *Thermodynamics of Small Systems* (Benjamin, New York, 1963, 1964), Vols. 1 and 2.
[10] N.A. Metropolis, A.W. Rosenbluth, M.N. Rosenbluth, A.H. Teller, and E. Teller, "Equation of state calculation by fast computing machines," *J. Chem. Phys.*, **21**, 1087 (1953).
[11] D.J. Adams, "Chemical potential of hard-sphere fluids by Monte Carlo methods," *Mol. Phys.*, **28**, 1241 (1974).
[12] B. Widom, "Some topics in the theory of fluids," *J. Chem. Phys.*, **39**, 2808 (1963).
[13] J. Kolafa, "Autocorrelations and subseries averages in Monte Carlo simulations," *Mol. Phys.*, **59**, 1035 (1986).
[14] L.T. Wille, "Close packing in curved space by simulated annealing," *J. Phys. A: Math. Gen.*, **20**, L1211 (1987).
[15] N.F. Carnahan and K.E. Starling, "Equation of state for nonattracting rigid spheres," *J. Chem. Phys.*, **51**, 635 (1979).